Submitted to *Applied Physics Letters*

Thermal Conduction Inhomogeneity of Nanocrystalline Diamond Films by Dual-Side Thermoreflectance

Elah Bozorg-Grayeli[1,a)], Mehdi Asheghi[1], Vincent Gambin[2], Rajinder Sandhu[2], Tatyana I. Feygelson[3], Bradford B. Pate[4], Karl Hobart[4], and Kenneth E. Goodson[1]

[1]Department of Mechanical Engineering, Stanford University, Stanford, CA, 94305

[2]Northrop Grumman Corporation, San Diego, CA, 92127

[3]Science Applications International Corporation, McLean, VA, 22102

[4]Naval Research Laboratory, Washington, DC, 20375

Abstract

Thin diamond films of thickness near one micrometer can have highly nonuniform thermal conductivities owing to spatially-varying disorder associated with nucleation and grain coalescence. Here we extract the nonuniformity for nanocrystalline CVD diamond films of thickness 0.5, 1.0, and 5.6 μm using picosecond thermoreflectance from both the top and bottom diamond surfaces, enabled by etching a window in the silicon substrate. The thermal conductivities vary from less than 100 W m^{-1} K^{-1} to more than 1300 W m^{-1} K^{-1} and suggest that the most defective material is confined to within one micrometer of the growth surface.

.

[a)]Electronic mail: ebozorgg@stanford.edu

Report Documentation Page

Form Approved
OMB No. 0704-0188

1. REPORT DATE	2. REPORT TYPE	3. DATES COVERED
2013		**00-00-2013 to 00-00-2013**

4. TITLE AND SUBTITLE	5a. CONTRACT NUMBER
Thermal Conduction Inhomogeneity of Nanocrystalline Diamond Films by Dual-Side Thermoreflectance	5b. GRANT NUMBER
	5c. PROGRAM ELEMENT NUMBER
6. AUTHOR(S)	5d. PROJECT NUMBER
	5e. TASK NUMBER
	5f. WORK UNIT NUMBER
7. PERFORMING ORGANIZATION NAME(S) AND ADDRESS(ES) **Stanford University ,Department of Mechanical Engineering,Stanford,CA,94305**	8. PERFORMING ORGANIZATION REPORT NUMBER
9. SPONSORING/MONITORING AGENCY NAME(S) AND ADDRESS(ES)	10. SPONSOR/MONITOR'S ACRONYM(S)
	11. SPONSOR/MONITOR'S REPORT NUMBER(S)

12. DISTRIBUTION/AVAILABILITY STATEMENT
Approved for public release; distribution unlimited

13. SUPPLEMENTARY NOTES
Applied Physics Letters, accepted and in press

14. ABSTRACT
Thin diamond films of thickness near one micrometer can have highly nonuniform thermal conductivities owing to spatially-varying disorder associated with nucleation and grain coalescence. Here we extract the nonuniformity for nanocrystalline CVD diamond films of thickness 0.5, 1.0, and 5.6 μm using picosecond thermoreflectance from both the top and bottom diamond surfaces, enabled by etching a window in the silicon substrate. The thermal conductivities vary from less than 100 W m-1 K-1 to more than 1300 W m-1 K-1 and suggest that the most defective material is confined to within one micrometer of the growth surface.

15. SUBJECT TERMS

16. SECURITY CLASSIFICATION OF:			17. LIMITATION OF ABSTRACT	18. NUMBER OF PAGES	19a. NAME OF RESPONSIBLE PERSON
a. REPORT	b. ABSTRACT	c. THIS PAGE			
unclassified	**unclassified**	**unclassified**	**Same as Report (SAR)**	**10**	

Diamond is viewed as a promising potential successor to Si and SiC as a thermal spreader for high electron mobility transistors (HEMT) based on GaN[1-5]. Since the 1980's, chemical vapor deposition of diamond has become well established[6-11] and has led to routine deposition of polycrystalline and nanocrystalline diamond thin films. A remaining challenge is to integrate diamond materials into high power device structures in order to take advantage the high thermal conductivity. Diamond thin film deposition requires a seed layer to nucleate film growth on a foreign substrate. In this work, the seeds are nanodiamonds (typically 5-10 nm diamond particles) spread at roughly 10^{12} seeds/cm^2 on the silicon substrate before growth. During the initial stage of deposition, the seed layer coalesces into a continuous film. The deposited film is fully coalesced at 300nm thickness. Beyond the initial coalescence layer, there is predominantly columnar growth normal to the silicon-diamond interface[11]. Unfortunately, if the thermal resistance due to the film coalescence layer is sufficiently large, diamond thin films with a coalescence layer between the bulk diamond film and the heat source may not offer a thermal advantage over Si or SiC[19,20].

Theoretically, isotopically-enriched single-crystal diamond might eventually offer thermal conductivities up to 5000 W m^{-1} K^{-1} at room temperature, and experiments on isotopically-enriched diamond have shown thermal conductivity as high as 3300 W m^{-1} K^{-1} [12-14]. For polycrystalline diamond films less than several hundred micrometers thick, the cross-plane thermal conductivity remains near 1000 W m^{-1} K^{-1} at room temperature[15,16]. Several factors impede the mean free path of phonons in these polycrystalline diamond films, reducing the intrinsic thermal conductivity. These include impurity scattering, grain boundary scattering, and interface scattering[15-18]. At the initial stage of diamond thin film deposition, these scattering sites are abundant, significantly reducing thermal conductivity[18]. This coalescence region is buried

underneath several μm of columnar diamond grains, making the thermal properties difficult to access. Since the coalescence region strongly affects the diamond thermal performance, it is critical to develop a technique which can extract the thermal properties of both the coalescence and columnar diamond region.

Here we perform picosecond time-domain thermoreflectance (TDTR) measurements on suspended nanocrystalline diamond films from 0.5 μm to 5.6 μm in thickness. By probing both sides of the suspended film, we capture the cross-plane thermal conductivity of both the coalescence region (k_C) and the high-quality columnar grain (k_{HQ}) regions. Using these results with a two-layer heat diffusion model of the diamond film, we estimate the thickness of the low conductivity coalescence layer and compare the thermal resistances of the coalescence versus high-quality regions. This analysis demonstrates that the coalescence region can be a substantial contributor to thermal resistance in a diamond thin film.

Picosecond TDTR uses the temperature-dependent optical properties of a thin metal transducer as a thermometer for a heated thin film stack[21,22]. Our TDTR system uses a passively-modelocked Nd:YVO_4 laser with 9.2 ps pulsewidth and 82 MHz repetition rate[23,24]. We then use a radially-symmetric model of heat diffusion through a multilayer stack to fit for the transducer-film thermal boundary resistance (TBR), the intrinsic thermal conductivity of the film, and the film-substrate TBR[26,27].

The heat capacitance of the diamond coalescence region is small compared to the total heat capacitance of the diamond film, and the coalescence region is several μm from the transducer film. As a result, the additional coalescence layer thermal resistance is impossible to extract separately from the diamond-silicon thermal boundary resistance[20]. In order to separate

the two properties, we require direct contact between the transducer layer and the coalescence layer. This involves removal of the silicon substrate to allow deposition of a metal transducer directly on the seeded surface of the coalescence region. To accomplish this, we deposited three nanocrystalline diamond films on silicon substrates of thicknesses 0.5 μm, 1.0 μm, and 5.6 μm. The silicon substrates were selectively etched to produce a suspended diamond thin film of roughly 5 μm in diameter. A 50 nm Al transducer layer was deposited on each side of the suspended diamond film (fig. 1).

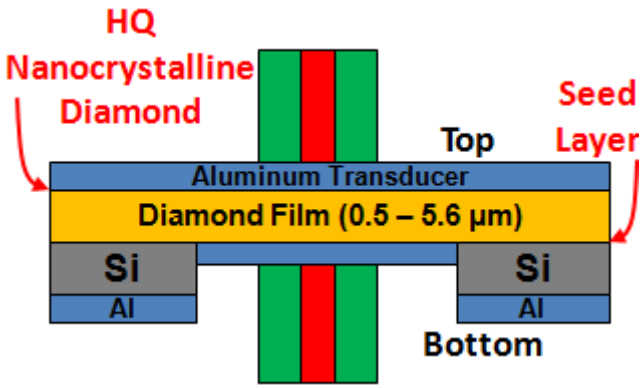

FIG. 1. Cross-sectional diagram of the suspended diamond film sample showing the Al transducer interface with the seeding/coalescence layer and with the high-quality (HQ) nanocrystalline diamond surface. Note that silicon has been etched to give access to the seeded surface of the diamond film where film coalescence occurs. The Al transducer layer is 50 nm thick, and the etched hole in silicon is ~ 5 mm in diameter. The red and green areas (color image available online) indicate the probe and pump beams, respectively.

When the characteristic thermal decay time of the film of interest is less than the measurement time scale, and the film is effectively insulated during the measurement time scale, the temperature decay of the transducer film depends primarily on the heat capacity and total thermal resistance of the film of interest. For the case of the 0.5 μm film, we obtain only an effective thermal resistance for the diamond film of 20 ± 2.0 m^2 K GW^{-1}, which can be expressed as:

$$R_{eff} = R_{Al-diam} + \frac{d_{diam}}{k_C} \quad (1)$$

where R_{eff} is the effective resistance of the diamond film, $R_{Al\text{-}diam}$ is the aluminum-diamond TBR, and d_{diam} is the thickness of the diamond film. We convert this to an effective thermal conductivity of the diamond layer by dividing the film thickness by the resistance. This gives a value of $k_{eff,C}$ of approximately 25 W m^{-1} K^{-1}. Using the previously reported diamond heat capacity[28] is ~ 2.15×10^{6} J m^{-3} K^{-1}, this translates to a total thermal diffusivity of ~ 1.16×10^{-5} m^{2} s^{-1}. The characteristic thermal decay time of the diamond, determined via:

$$\tau_{diam} = \frac{d_{diam}^2}{\alpha_{eff}} \quad (2)$$

where α_{eff} is the effective thermal diffusivity, is ~ 22 ns. The characteristic timescale of the heating event, however, is given by the inverse of the 5 MHz pump modulation frequency. This translates to a heating timescale of 200 ns, significantly greater than τ_{diam}. Therefore, although measurements on this sample are insensitive to the difference between intrinsic and thermal boundary resistance, we can uniquely extract the diamond heat capacity. The fitted heat capacity, 1.98×10^{6} J m^{-3} K^{-1}, is similar to previous literature results[28].

In order to separate out k_C and $R_{Al\text{-}diam}$ from the effective thermal resistance, we use the 1.0 μm thick diamond film. While τ_{diam} for this film (~56 ns) is still less than the timescale of the measurement, we have sufficient sensitivity to separate the transducer-film TBR from the intrinsic film thermal conductivity. Modeling the system as 50 nm Al on 1.0 μm diamond, we extract a TBR of 13.5 ± 1.0 m^{2} K GW^{-1} between the Al transducer and the diamond coalescence layer. Further, we find a cross-plane thermal conductivity of 80 ± 10 W m^{-1} K^{-1} for the diamond coalescence layer. By applying these results to equation (1), and setting d_{diam} to 0.5 μm, we

obtain a total thermal resistance that agrees with the value measured from the 0.5 μm diamond sample. Comparing the results with the model of local diamond thermal conductivity developed by Touzelbaev et al indicates an average coalescence layer grain size of 100-200 nm[18].

We determine the thickness of the thermally resistive coalescence layer using the 5.6 μm diamond film. Picosecond TDTR measurements on the top side of the diamond reveal an Al-diamond thermal boundary resistance of 10.7 ± 1.0 m^2 K GW^{-1}, smaller than for the Al-coalescence layer interface. Since the thermal boundary resistance is highly dependent on surface cleanliness, this difference may be due to impurities left behind by the etching process on the bottom diamond film surface. Assuming the heat capacity measured from the 0.5 μm sample, and using a one-layer model of 50 nm Al on 5.6 μm diamond, we find a cross-plane thermal conductivity of 1350 ± 200 W m^{-1} K^{-1} for the high-quality diamond (fig. 2). It is worth noting that the result of the numerical fit for this sample remains the same even assuming a diamond thickness as low as 2.5 μm. This implies the top side measurement may be insensitive to the coalescence layer properties.

To confirm this hypothesis, we performed TDTR on the bottom of the same sample. Figure 3 demonstrates the difference in the thermoreflectance curves for the two measurements, showing a significantly slower thermal decay through the coalescence-layer. Using the coalescence layer diamond data from the 5.6μm thick film, we created a two-layer model of heat conduction through the suspended film. This model assumes 50 nm of Al on a diamond coalescence layer with unknown thickness, d_C, on a high-quality diamond layer of thickness d_{HQ} = 5.6 μm-d_C. Assuming k_C = 80 W m^{-1} K^{-1} and k_{HQ} = 1350 W m^{-1} K^{-1}, we fit for the coalescence layer thickness and find d_C = 0.76 ± 0.1 μm. The thickness of the high quality diamond layer, therefore, is ~4.84 μm, thick enough to render the top side measurements insensitive to the

thermal properties of the coalescence layer diamond. This validates the one-layer assumption used for the top side measurement of the 5.6 μm sample.

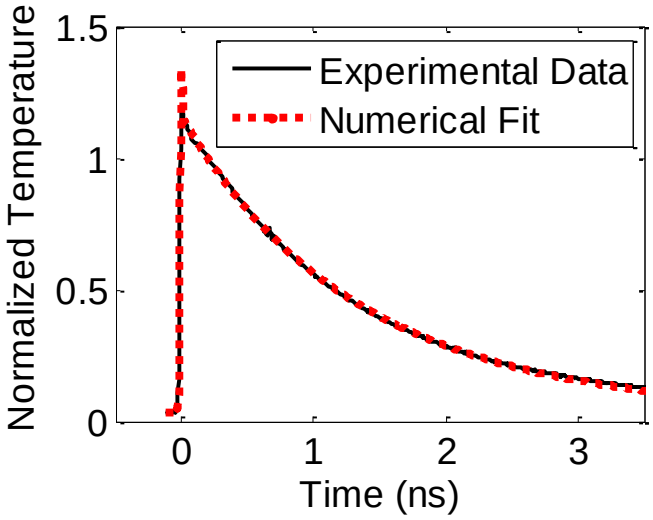

FIG. 2. Picosecond TDTR data (solid line) and numerical fit (dotted line) for the top side measurement of the 5.6 μm diamond film. The fit corresponds to an Al-diamond thermal boundary resistance of 10.7 ± 1.0 m^2 K GW^{-1} and a diamond thermal conductivity of 1350 ± 200 W m^{-1} K^{-1}.

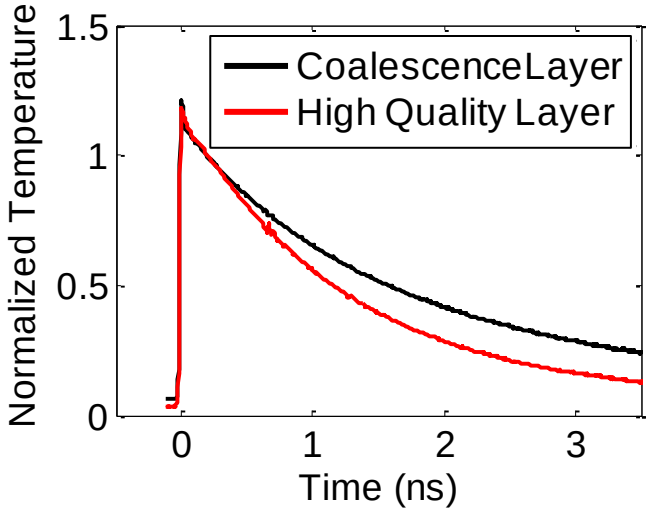

FIG. 3. Comparison of picosecond TDTR curves from the coalescence and high quality layers of the 5.6 μm diamond sample. The larger, higher quality diamond grains on the top surface result in a higher thermal conductivity than for the bottom. This is evidenced by the faster thermal decay shown for the high quality layer.

The thickness prediction for the coalescence layer is more subtle than the two-layer model implies. Although the diamond film consists of columnar grains on a thin coalescence

layer, there is no sharp transition between the two. Rather, the average grain size in the film increases smoothly as a function of distance from the substrate surface. What the two-layer model determines is an estimated thickness based on the thermal conductivity measured in the thinner samples. If we assume a higher thermal conductivity, the fitted coalescence layer thickness increases proportionally. A more robust comparison would involve the thermal resistances of the two layers. Although the fitted thickness of the coalescence layer depends proportionally on the assumed thermal conductivity, the fitted thermal resistance of the layer remains the same regardless of assumed thermal conductivity.

The thermal properties of the diamond film coalescence layer have a drastic effect on the total thermal resistance of the film. Using the coalescence layer thickness and thermal conductivity we estimated using the two-layer model, we find, for a 5.6 μm diamond film, that the coalescence layer thermal resistance ($R_C = d_C/k_C$) is ~ 9.5 ± 1.4 m^2 K GW^{-1}. This is significantly larger than the thermal resistance of the rest of the diamond film (~ 3.6 ± 0.6 m^2 K GW^{-1} assuming a 0.76 μm coalescence layer). In fact, the coalescence layer has a thermal resistance equivalent to ~ 12.8 μm of high quality diamond.

This work extracts the thermal conductivity nonuniformity in nanocrystalline diamond films of thickness near 5 micrometers using dual-sided picosecond TDTR measurements. This technique extracted the thermal conductivity of the coalescence layer, the high quality diamond layer, and the heat capacity of the suspended films. From these results, we estimate the coalescence layer thickness and calculate the thermal resistance contributions of both regions of the diamond film. The additional coalescence layer thermal resistance is significant. Further research into nanocrystalline diamond nucleation and growth may improve the coalescence layer

thermal properties, reducing the total thermal resistance and enhancing the thermal performance of integrated nanocrystalline diamond thermal spreaders for high-power transistor applications.

ACKNOWLEDGMENT

Special thanks are due to Aditya Sood at Stanford University for his assistance in preparing samples during the primary author's absence. This research was made with Private and Government support under and awarded by Northrop Grumman (agreement # 7600011363, titled: Thermal Reflectance Material Characterization Supporting the NEXT Program Phase I&II), DARPA (agreement # FE 01 19 12, titled: GaN-on-Diamond thermal measurements and agreement # RFMD-12-C-0002, titled: Thermal Characterization of GaN-on-Diamond Materials and PA Devices), and the AFOSR (agreement # FA9550-12-1-0195, titled: MultiCarrier and Low-Dimensional Thermal Conduction at Interfaces for High Power Electronic Devices).

REFERENCES

[1] G. H. Jessen, J. K. Gillespie, G. D. Via, A. Crespo, D. Langley, J. Wasserbauer, F. Faili, D. Francis, D. Babic, F. Ejeckam, S. Guo, and I. Eliashevich, in *AlGaN/GaN HEMT on Diamond Technology Demonstration*, 2006, p. 271-274.

[2] J. G. Felbinger, M. V. S. Chandra, S. Yunju, L. F. Eastman, J. Wasserbauer, F. Faili, D. Babic, D. Francis, and F. Ejeckam, Electron Device Letters, IEEE **28,** 948-950 (2007).

[3] Q. Diduck, J. Felbinger, L. F. Eastman, D. Francis, J. Wasserbauer, F. Faili, D. I. Babic, and F. Ejeckam, Electronics Letters **45,** 758-759 (2009).

[4] M. J. Tadjer, T. J. Anderson, K. D. Hobart, T. I. Feygelson, J. D. Caldwell, C. R. Eddy, F. J. Kub, J. E. Butler, B. Pate, and J. Melngailis, Electron Device Letters, IEEE **33,** 23-25.

[5] C. Jungwan, L. Zijian, E. Bozorg-Grayeli, T. Kodama, D. Francis, F. Ejeckam, F. Faili, M. Asheghi, and K. E. Goodson, in *Thermal characterization of GaN-on-diamond substrates for HEMT applications*, p. 435-439.

[6] J. C. Angus, H. A. Will, and W. S. Stanko, Journal of Applied Physics **39,** 2915-2922 (1968).

[7] B. V. Spitsyn, L. L. Bouilov, and B. V. Derjaguin, Journal of Crystal Growth **52, Part 1,** 219-226 (1981).

[8] M. Kamo, Y. Sato, S. Matsumoto, and N. Setaka, Journal of Crystal Growth **62,** 642-644 (1983).

[9] Y. Hirose and Y. Terasawa, Japanese Journal of Applied Physics **25,** L519-L521 (1986).

[10] M. Kamo, H. Yurimoto, and Y. Sato, Applied Surface Science **33-34,** 553-560 (1988).

[11] J. Philip, P. Hess, T. Feygelson, J. E. Butler, S. Chattopadhyay, K. H. Chen, and L. C. Chen, Journal of Applied Physics **93,** 2164-2171 (2003).

[12] G. A. Slack, Journal of Applied Physics **35,** 3460-3466 (1964).

[13] T. R. Anthony, W. F. Banholzer, J. F. Fleischer, L. Wei, P. K. Kuo, R. L. Thomas, and R. W. Pryor, Physical Review B **42,** 1104-1111 (1990).
[14] L. Wei, P. K. Kuo, R. L. Thomas, T. R. Anthony, and W. F. Banholzer, Physical Review Letters **70,** 3764-3767 (1993).
[15] J. E. Graebner, S. Jin, G. W. Kammlott, J. A. Herb, and C. F. Gardinier, Nature **359,** 401-403 (1992).
[16] D. T. Morelli, C. P. Beetz, and T. A. Perry, Journal of Applied Physics **64,** 3063-3066 (1988).
[17] K. E. Goodson, O. W. Käding, M. Rösler, and R. Zachai, Journal of Applied Physics **77,** 1385-1392 (1995).
[18] M. N. Touzelbaev and K. E. Goodson, Journal of Thermophysics and Heat Transfer **11,** 506-512 (1997).
[19] A. Aminfar, E. Bozorg Grayeli, M. Asheghi, and K. E. Goodson, in *Analysis of HEMT multilayered structures using a 2D finite volume model*, 2012, p. 224-234.
[20] E. Bozorg-Grayeli, L. Zijian, V. Gambin, M. Asheghi, and K. E. Goodson, in *Thermal conductivity, anisotropy, and interface resistances of diamond on poly-AlN*, 2012, p. 1059-1064.
[21] K. Ujihara, Journal of Applied Physics **43,** 2376-2383 (1972).
[22] C. A. Paddock and G. L. Eesley, Journal of Applied Physics **60,** 285-290 (1986).
[23] M. A. Panzer, M. Shandalov, J. A. Rowlette, Y. Oshima, C. Yi Wei, P. C. McIntyre, and K. E. Goodson, Electron Device Letters, IEEE **30,** 1269-1271 (2009).
[24] J. P. Reifenberg, K.-W. Chang, M. A. Panzer, S. Kim, J. A. Rowlette, M. Asheghi, H.-S. P. Wong, and K. E. Goodson, IEEE Electron Device Letters **31,** 56-58 (2010).
[25] A. J. Schmidt, X. Chen, and G. Chen, Review of Scientific Instruments **79,** 114902-9 (2008).
[26] A. Feldman, High Temperatures - High Pressures **31,** 293-298 (1999).
[27] D. G. Cahill, Review of Scientific Instruments **75,** 5119-5122 (2004).
[28] A. C. Victor, The Journal of Chemical Physics **36,** 1903-1911 (1962).